A theoretical investigation of the near UV and VIS electronic spectra for the fully deprotonated forms of anhydrotetracycline

Wagner B. De Almedia,*[a,b] Luís Ricardo A. Costa,[a] Hélio F. Dos Santos[a] and Michael C. Zerner[b]

[a] *Laboratório de Química Computacional e Modelagem Molecular (LQC-MM), Departamento de Química, ICEx, UFMG, Belo Horizonte, MG, 31270-901, Brazil*
[b] *Quantum Theory Project, University of Florida, Gainesville, Florida, 32611-8435, USA*

Anhydrotetracycline (AHTC) is the major toxic decomposition product of the antibiotic tetracycline with a characteristic electronic spectrum used for identification purposes. In the present work, the electronic spectra of the fully deprotonated forms (L^{2-}) of the free AHTC molecule, the main species involved in the metal complexation reaction, have been analysed using the spectroscopic version of the INDO/S method. The polarization and specific solute–solvent interaction were analysed using the standard SCRF continuum model and the supermolecule approach. The theoretical band spectra were simulated by fitting the calculated frequency and oscillator strength values to a Lorentzian type function and directly compared with the experimental aqueous solution spectrum. For the L^{2-}(10-O) deprotonated molecule, the theoretical spectrum in the near UV region showed three absorption bands located at 215, 261 and 336 nm, which are in very good agreement with the observed values: 220, 268 and 335 nm. All transitions were assigned as $\pi\rightarrow\pi^*$ of the BCD ring chromophore with contributions of the A ring for the absorption at 261 nm. The same transitions were located at 222 and 261 nm for the L^{2-}(11-O) and the shoulder at 236 nm is not observed.

Introduction

The anhydrotetracycline (AHTC, Fig. 1) is the major toxic decomposition product of the tetracycline (TC) parent compound, an important representative member of a group of widely used antibiotics.[1] The AHTC derivative is responsible for several side-effects of the drug, such as the reversible Fanconi type syndrome and cutaneous phototoxicity upon ingestion of TC beyond its limit of validity.[2,3] The loss of activity of the anhydrous compound is attributed to the aromatization of the C ring and change in the conformation of A ring. Solid state studies[4] of the fully protonated form of the TC molecule show a twisted conformation, in which H(4-N) is hydrogen bonded to 3-O. For the protonated form of AHTC derivative (LH_3^+) an extended conformation was observed in the solid state,[4] with a hydrogen bond between H(4-N) and 12a-O. In the structure–activity analysis of some TC derivatives (including AHTC) the same twisted structure for all biologically active compounds in the solid state was observed,[4] suggesting that conformation as the preferred one for biological activity. Experimental studies in water solution[3,5] showed that the conformation changes depending on pH of the medium.

Circular dichroism (CD) studies of TC[5] suggest the presence of a twisted conformer at pH < 8 and an extended conformation at pH > 8. The same results have been obtained for the AHTC molecule using CD spectroscopy,[3] showing that the change in the conformation of the A ring, observed in solid state, is not the only factor to be considered for biological activity. The conformational change from twisted to extended at pH > 8 can be understood by analysing the ionized species present in the medium. At that pH, the molecule is fully deprotonated (L^{2-}) and it is stabilized by a hydrogen bond between 12a-OH and 4-N. At pH < 8, the totally protonated (LH_3^+), the zwitterionic ($LH_2^{\pm}$) and the partial ionized (LH^-) species are stabilized by a hydrogen bond between H(4-N) and 3-O. The order of acidity, according to potentiometric studies,[2,3] is: H(3-O) > H(10-O) or H(11-O) > H(4-N). The second deprotonation site is attributed to the H(10-O).[2] However, there is IR spectroscopic evidence[2] that the carbonyl at 12-C and 11-O are involved in the coordination with some metals, which suggests the tautomeric equilibrium 11-O · · · H · · · 10-O.

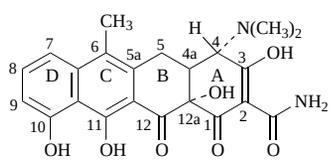

Fig. 1 Numbering scheme of the AHTC molecule

In this work we have analysed the electronic spectra of the two fully deprotonated forms of the AHTC molecule named L^{2-}(10-O) and L^{2-}(11-O), where the labels in parentheses indicate the respective deprotonation site (see Fig. 1). The main goal of this study is to develop a systematic analysis of the theoretical absorption spectra of the free ligand AHTC in the form which it is involved in the metal complexation process. The solvent effect will be discussed in two different approaches: the standard self consistent reaction field (SCRF) continuum model and the supermolecule (SM) approach. It is the first step towards the study of the complexation reaction through investigation of the electronic spectra which characterizes these reactions.

Calculation

In previous work,[6] we have developed a systematic conformational analysis of every ionized form of the AHTC molecule. The AM1 gas phase geometries for the extended conformer of the L^{2-} species, obtained in that study, are shown in Fig. 2. These geometries were used to calculate the electronic spectra using the ZINDO program, where a spectroscopic version of the INDO/S method, as parametrized by Zerner and coworkers, is implemented.[7] The solvent effect was, in a first approximation, included using the SCRF ($\varepsilon = 78.54$) formulation as given by Karelson and Zerner[8] with inclusion of the quadrupole term in the electrostatic potential expansion. In a second step, the effect in the absorption spectra due to specific solute–solvent interaction was analysed using the supermole-

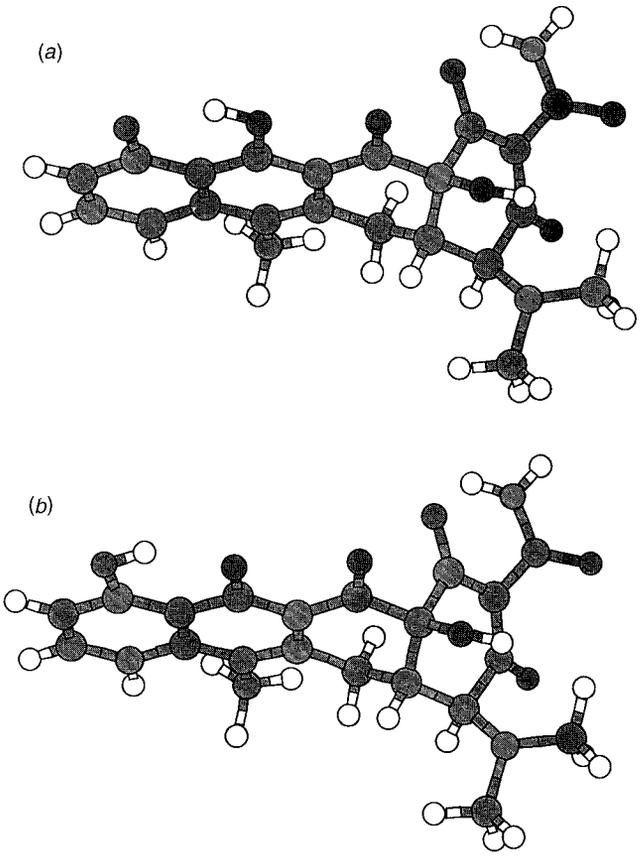

Fig. 2 AM1 optimized structures of the fully deprotonated forms of the AHTC molecule, L^{2-}(10-O) (*a*) and L^{2-}(11-O) (*b*)

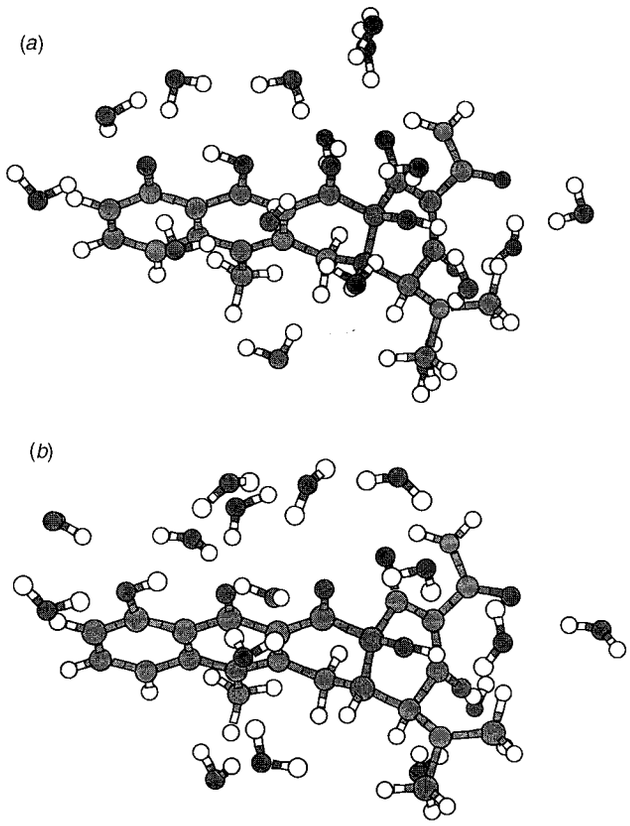

Fig. 3 Three-dimensional representation of the supermolecules obtained from Monte-Carlo simulation, L^{2-}(10-O)·16H_2O (*a*) and L^{2-}(11-O)·16H_2O (*b*)

cule (SM) approach. The supermolecules were constructed using the Monte-Carlo method as implemented in the BOSS version 3.5 program.[9] 100 water molecules were used in the simulations and 500 000 configurations were generated for the system equilibration. The simulations were carried out at 20 °C and 1 atm and the solute and solvent structures were frozen during the simulation. For the electronic spectra calculations, the last configuration obtained in the simulation procedure was used and only 16 water molecules were explicitly considered, which were selected according to the solute–solvent interaction energy. The supermolecule structures obtained are shown in Fig. 3. The combined treatment (SM + SCRF) was also investigated at the end, where 16 water molecules were considered explicitly and the solvent bulk was simulated using the SCRF continuum model. In all solvent approaches employed in this work the gas phase geometries were used.

The band spectra simulation

All electronic spectra were obtained using a configuration interaction (CI) calculation including all single excitations from the 16 highest occupied molecular orbitals (MO) to the 16 lowest unoccupied MO. A total of 257 configurations were generated.

The wavelength (λ) and oscillator strength (f) values, calculated using the spectroscopic INDO/S approach, were used in the simulation of the band spectra. The band shapes were described by a Lorentzian type function[10] [eqn. (1)], where $\varepsilon(\nu)$

$$\varepsilon(\bar{\nu}) = \varepsilon_{max}(\bar{\nu}_{max}) \frac{(\Delta\bar{\nu}_{1/2})^2/4}{(\Delta\bar{\nu}_{1/2})^2/4 + (\bar{\nu} - \bar{\nu}_{max})^2} \quad (1)$$

(in $dm^3\ mol^{-1}\ cm^{-1}$) is the extinction coefficient at the frequency ν (in cm^{-1}) and $\Delta\nu_{1/2}$ (in cm^{-1}) is the width of the peak at half height. The dimensionless quantity f is given by[10] [eqn. (2)],

$$f = 4.33 \times 10^{-9} \int_0^\infty \varepsilon(\bar{\nu}) d\bar{\nu} \quad (2)$$

where the integral is the integrated absorption coefficient and represents the area under an absorption band when ε is plotted against ν. Using eqn. (1) and (2) it is possible to obtain an expression which relates to the oscillator strength (f) with the maximum absorption coefficient (ε_{max}) [eqn. (3)].

$$\varepsilon_{max} = \frac{4f}{\pi\Delta\bar{\nu}_{1/2} 4.33 \times 10^{-9}} \quad (3)$$

Each band was adjusted separately and the total spectrum was determined by eqn. (4), where the summation is over all

$$\varepsilon(\bar{\nu}) = \sum_i \varepsilon_i(\bar{\nu}) \quad (4)$$

absorptions *i*, at the frequency ν. As a first approximation, in this work the width of the peak at half height was considered to be constant (equal to 6000 cm^{-1}) in the entire spectral range (200–800 nm) investigated.

Results and discussion

The calculated electronic transitions for the L^{2-}(10-O) and L^{2-}(11-O) molecules are presented in Tables 1 and 2, respectively. The values of wavelength (λ) and oscillator strengths (f) obtained in the gas phase and water solution, using different approaches, are reported.

Analysing the visible (VIS) portion of the spectrum ($380 < \lambda < 780$ nm), it can be noted that only one transition was observed in the gas phase for the L^{2-}(10-O) species (382 nm) and two for the L^{2-}(11-O) compound (400 and 381 nm). The lowest energy absorptions for each molecule (382 and 400 nm) are due to the electronic transition from HOMO to LUMO and, according to the MO symmetry, it was assigned as a $\pi\rightarrow\pi^*$ transition of the BCD ring chromophore (see Fig. 1). The absorption at 381 nm [L^{2-}(11-O)] is attributed to a transition

Table 1 Calculated absorption spectra for the fully deprotonated form of AHTC molecule, L^{2-}(10-O), in gas phase and water solution. The solvent effect was included using the standard SCRF model and supermolecules approaches (SM and SM + SCRF).

Gas			SCRF(ε = 78.54)			SM			SM + SCRF(ε = 78.54)			
λ/nm	f [a]	CI contribution [b]	λ/nm	f [a]	CI contribution [b]	λ/nm	f [a]	CI contribution [b]	λ/nm	f [a]	CI contribution [b]	Attribution [c]
382	0.501	91%(81→82)	397	0.127	51%(77→82)	391	0.483	90%(145→146)	382 [d]	0.451	81%(145→146)	π→π*(R)
351	0.106	80%(81→83)	351	0.288	45%(77→83)	353	0.107	81%(145→147)	336 [e]	0.121	69%(145→147)	π→π*(R)
266	0.236	76%(80→84)	245	0.284	67%(81→92)	268	0.308	81%(144→148)	280 [f]	0.151	62%(144→148)	π→π*(A)
261	0.353	28%(81→85)	276	0.237	78%(75→82)	261	0.450	23%(143→146)				π→π*(R)
			245	0.312	48%(75→83)				244 [f]	0.130	72%(143→147)	π→π*(R)
259	0.214	53%(80→86)	294	0.112	61%(81→89)	257	0.136	59%(144→150)	263 [f]	0.243	25%(144→149)	π→π*(A)
									260 [f]	0.393	22%(144→149)	π→π*(A)
			226	0.466	24%(71→83)							π→π*(R)
212	0.456	44%(75→83)	217	0.391	34%(71→83)	214	0.197	14%(139→147)	213 [g]	0.362	40%(140→147)	π→π*(R)
						211	0.378	18%(139→147)				π→π*(R)

[a] Oscillator strengths. [b] Only the main CI contribution has been considered. 81 is the HOMO of AHTC, and 145 is the HOMO of SM = AHTC·16H_2O. [c] The abbreviations R and A stand for BCD ring chromophore and A ring respectively (see Fig. 1). Observed absorptions in basic water solution [3]: λ_{max}/nm (ε_{max}/dm^3 mol^{-1} cm^{-1}). [d] 430 (10 400). [e] 335 (4600). [f] 268 (39 800). [g] 220 (25 000).

Table 2 Calculated absorption spectra for the fully deprotonated form of AHTC molecule, L^{2-}(11-O), in gas phase and water solution. The solvent effect was included using the standard SCRF model and supermolecule approaches (SM and SM + SCRF).

Gas			SCRF(ε = 78.54)			SM			SM + SCRF(ε = 78.54)			
λ/nm	f [a]	CI contribution [b]	λ/nm	f [a]	CI contribution [b]	λ/nm	f [a]	CI contribution [b]	λ/nm	f [a]	CI contribution [b]	Attribution [c]
400	0.439	81%(81→82)	440	0.473	56%(80→82)	399	0.398	87%(145→146)	401 [e]	0.402	88%(145→146)	π→π*(R)
381	0.102	82%(81→83)				374	0.154	89%(145→147)	381	0.137	92%(145→147)	π→π*(R)
266	0.142	26%(81→87)	255	0.103	50%(80→87)	274	0.115	59%(145→150)	275 [f]	0.128	62%(145→151)	π→π*(R)
			247	0.294	44%(75→83)	261 [d]	0.050	26%(145→148)	261 [f]	0.100	34%(145→150)	π→π*(R)
265	0.138	54%(80→84)	248	0.515	44%(81→91)	264	0.216	67%(144→149)	264 [d,f]	0.074	28%(144→148)	π→π*(A)
258	0.312	29%(80→86)	290	0.134	46%(81→89)	257	0.222	44%(144→151)	257 [f]	0.213	46%(144→149)	π→π*(A)
214	0.437	24%(75→83)	223 [d]	0.070	58%(70→82)	219	0.228	40%(145→154)	220 [g]	0.280	42%(145→154)	π→π*(R)
214	0.341	25%(75→83)										π→π*(R)

[a] Oscillator strengths. [b] Only the main CI contribution has been considered. See Table 1. [c] The abbreviations R and A stand for BCD ring chromophore and A ring, respectively (see Fig. 1). [d] No transitions with f > 0.1 were observed in that region. Observed absorptions in basic water solution [3]: λ_{max}/nm (ε_{max}/dm^3 mol^{-1} cm^{-1}). [e] 430 (10 400). [f] 268 (39 800). [g] 220 (25 000).

from HOMO to LUMO + 1. This transition was observed in the L^{2-}(10-O) electronic spectrum at 351 nm and assigned as a π→π* of the BCD conjugated ring system. A red shift was observed, in this region, for both molecules studied, when the solvent was included by the SCRF continuum model. In this approach, the HOMO is located at the A ring (Fig. 1) and does not take part in the transition. The specific interaction solvent effect can be seen from the results obtained in the SM calculation. A small bathochromic shift was observed in the L^{2-}(10-O) molecule and no significative change in the corresponding band position was obtained for the L^{2-}(11-O) compound. In the combined treatment (SM + SCRF), the transition energies did not change in comparison with the gas phase values for both compounds. In general, a red shift was observed due to the tautomerization process [L^{2-}(10-O)→L^{2-}(11-O)] in all approaches employed.

The near ultraviolet (UV) spectrum range is more complex. For ease of discussion, it is divided into three distinct regions: (*i*) 200 < λ < 230 nm, (*ii*) 230 < λ < 300 nm and (*iii*) 300 < λ < 380 nm. In the (*i*) branch, it can be seen from Tables 1 and 2, that the L^{2-}(10-O) deprotonated form exhibits one transition at 212 nm and the L^{2-}(11-O) molecule showed two degenerate absorptions at 214 nm attributed to a π→π* transition of the BCD chromophore. In all solvent models used, a small red shift was observed for both compounds, being that effect less pronounced when the supermolecule approaches (SM and SM + SCRF) were used.

The majority of the transitions are present in the second portion of the UV spectrum [(*ii*) branch]. In this region, contribution from MO of the BCD ring system and the A ring were observed. In the gas phase, three transitions are present for both molecules, located respectively at: 266, 261 and 259 nm [L^{2-}(10-O)] and 265, 266 and 258 nm [L^{2-}(11-O)] assigned respectively as π→π* (A ring), π→π* (BCD chromophore) and π→π* (A ring). The two transitions of the A ring contain contributions from different MOs. In the lowest energy one (266 and 265 nm), the MOs involved are located on the A ring and the other one (259 and 258 nm) has the contribution from the MO primarily located near the amide group (see Fig. 1). The polarization solvent effect (according to the SCRF model) changes the band positions significantly. The transitions of the A ring are shifted to 245 and 294 nm [L^{2-}(10-O)] and to 248 and 290 nm [L^{2-}(11-O)]. In the SM approach, no significant changes were observed for both compounds (see Table 1 and 2). However, when the polarization effect is included in the SM calculation (SM + SCRF) the transition at 266 nm [L^{2-}(10-O)] is shifted to 280 nm. No significant modifications were observed for the L^{2-}(11-O) species.

The last UV range to be analysed is the (*iii*) branch (300 < λ < 380 nm). In this region only one absorption was observed for the L^{2-}(10-O) compound at 351 nm (gas phase). As mentioned before, the corresponding transition was observed in the VIS spectrum range at 381 nm for the L^{2-}(11-O) molecule. These transitions were attributed to a π→π* excitation of the BCD ring system. For the L^{2-}(10-O) deprotonated form, no shift was observed when the continuum model (SCRF) was considered. In the SM approach, this same transition was shifted to 353 nm [L^{2-}(10-O)] and the absorption at 381 nm [L^{2-}(11-O)] was shifted to 374 nm. In the SM + SCRF study, the band at 351 nm was blue shifted to 336 nm in the L^{2-}(10-O) electronic spectrum and no changes were observed for the L^{2-}(11-O) molecule relative to the values obtained in the gas phase. As in the VIS spectrum, a bathochromic effect was observed in the (*i*) and (*iii*) regions of the UV spectrum due to the tautomerization process.

The values of λ and f showed in Tables 1 and 2 are not

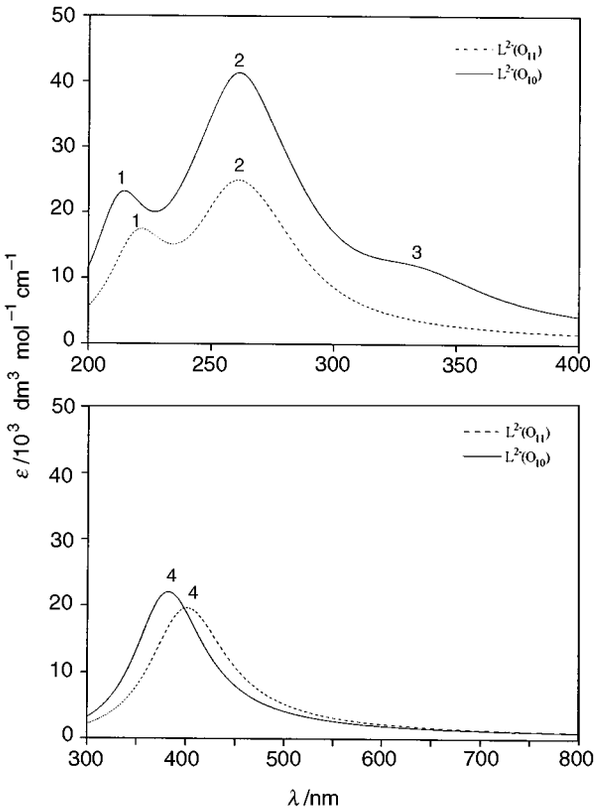

Fig. 4 Near UV (*a*) and VIS (*b*) spectra of the fully deprotonated forms of AHTC molecule, L^{2-}(10-O) (solid line) and L^{2-}(11-O) (segmented line). The simulations were done using the SM + SCRF($\varepsilon = 78.54$) approach. The absorption bands 1–4 are characterized in Table 3.

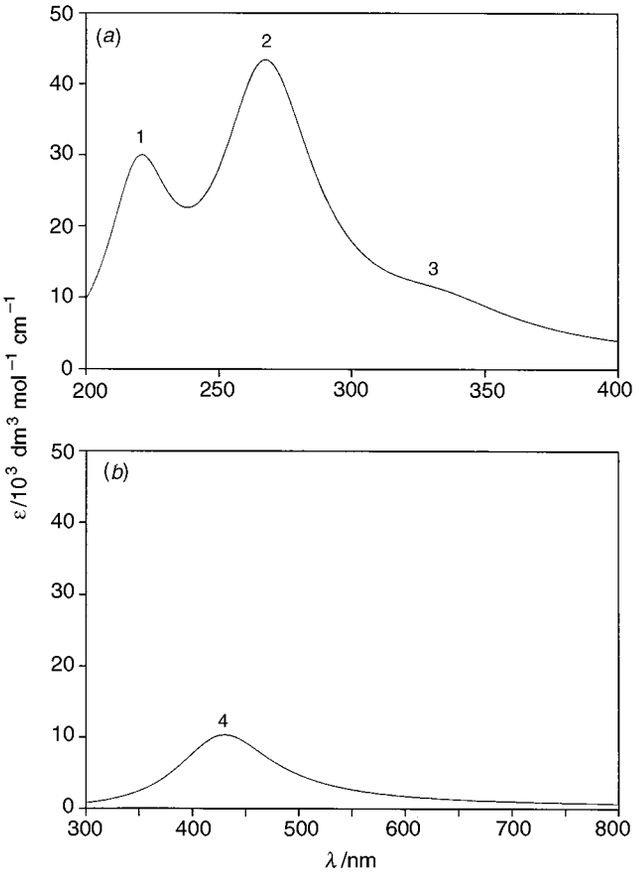

Fig. 5 Near UV (*a*) and VIS (*b*) experimental spectra of the AHTC molecule observed at pH = 10. The spectra were obtained using the simulation procedure described in the calculation section. The values of ε_{max} shown in Table 3 were used to calculate the oscillator strength f. The absorption bands 1–4 are characterized in Table 3.

directly compared with experiment. The real spectrum consists of an overlapping of many broad bands. In an attempt to represent the theoretical electronic spectrum as it is observed experimentally, the simulation procedure described in the calculation section was applied to the values of λ and f calculated using INDO/S method. Fig. 4 shows the calculated near UV and VIS spectra for the two fully deprotonated forms of the AHTC compound. These spectra were obtained using the SM+SCRF approach, taken as the most realistic description of the solvent effect in this work. In Fig. 5, the experimental spectra, obtained by applying the simulation procedure to the experimental data, are shown. Table 3 contains the values of λ_{max} and ε_{max} obtained from the simulation and observed experimentally.

The theoretical UV spectrum for the L^{2-}(10-O) molecule showed two bands centred at 215 and 261 nm and a shoulder at 336 nm, in good agreement with the experimental data: 220, 268 and 335 nm (shoulder). The intensity of the absorption at 336 nm is overestimated in comparison with experiment. The value of ε_{max} obtained in the simulation of the isolated band at 336 nm (see Table 1) was equal to 5929 dm^3 mol^{-1} cm^{-1}, in very good agreement with the corresponding experimental one ($\varepsilon_{max} = 4600$ dm^3 mol^{-1} cm^{-1}). The maximum absorption coefficient obtained after applying the simulation procedure to the experimental data ($\varepsilon_{max} = 11\,102$) shows that the discrepancy observed is a consequence of the simulation procedure and suggests that the use of a constant width at half height might be one of the factors responsible for the disagreement obtained. For the L^{2-}(11-O) compound, only two bands are observed in the UV spectrum, located at 222 and 261 nm. The shoulder appearing in the L^{2}(10-O) electronic spectrum was not found for the other tautomer. Comparing the two UV spectra obtained, a bathochromic shift of the band at 215 nm [L^{2-}(10-O)] and a hypochromic displacement of both band absorptions (215 and 261) due to the tautomerization process can be observed.

Table 3 Wavelength (λ_{max}/nm) and molar absorptivity (ε_{max}/dm^3 mol^{-1} cm^{-1}) obtained from the simulated electronic spectra of the fully deprotonated forms of AHTC molecule, L^{2-}(10-O) and L^{2-}(11-O). The calculation was done using the SM + SCRF approach.

Band[a]		L^{2-}(10-O)	L^{2-}(11-O)	Expt.[b,c]	Assignment[d]
1	λ_{max}	215	222	220 (221)	π→π*(R)
	ε_{max}	23 226	17 516	25 000 (30 016)	
2	λ_{max}	261	261	268 (267)	π→π*(R)
	ε_{max}	41 355	24 961	39 800 (43 435)	π→π*(A)
3	λ_{max}	336	—	335 (334)	π→π*(R)
	ε_{max}	11 860[e]	—	4 600 (11 102)	
4	λ_{max}	382	402	430 (429)	π→π*(R)
	ε_{max}	22 102	19 698	10 400 (10 388)	

[a] See Figs. 4 and 5. [b] Values from ref. 3. [c] The values in parentheses were obtained after applying the simulation procedure to the experimental data (see Fig. 5). [d] R and A stand for the BCD ring chromophore and the A, ring respectively (Fig. 1). [e] The value of ε_{max} obtained for isolated band at 336 nm was 5929 dm^3 mol^{-1} cm^{-1}.

In the VIS region, only one transition was considered in the simulation, and this was located at 382 [L^{2-}(10-O)] and 402 nm [L^{2-}(11-O)]. The same red shift and hypochromic effect was observed due to tautomerism. The band intensities are overestimated in relation to the experimental values, and the possible reason might be the same as discussed before. This absorption band is the most important in the complexation reaction. Experimentally, the complexation site is determined through the shift observed in that band from 430 nm to *ca.* 445 nm, depending on the metal used.[3]

Finally, it is important to make clear some relevant results of this study. From the good agreement between theoretical and experimental electronic spectrum, it can be said that the

extended conformations of the fully deprotonated forms of the AHTC compound are likely those present in the basic water solution, as suggested by CD and UV–VIS experimental studies.[3–5] Except for the shoulder at 336 nm in the L^{2-}(10-O) UV spectrum, the electronic spectra of the two tautomeric forms are very similar and, considering the equilibrium, the observed spectrum could well be the superposition of both. The solvent effect was best described by the supermolecule approach in the reaction field for both compounds studied. The reaction field, by itself, was not accurate enough to correctly describe the shape of the electronic spectra.[11,12] The description of the spectrum as a superposition of broadened transitions gives a very accurate representation of the experimental spectrum, one we believe can be used for the analysis of the AHTC in different environments.

Conclusions

The near UV and VIS electronic spectra for the fully deprotonated forms of AHTC molecule, were calculated using the semi-empirical spectroscopic version of the INDO/S method. The results obtained, using different approaches, for the gas phase and water solution species, were discussed, showing a very good agreement between theoretical and experimental solution spectra. The band spectra are accurately reproduced and the calculated values of λ_{max} and ε_{max} compare very well with experimental data.

These results strongly suggest that the extended conformation of the AHTC compound should make the major contribution in basic water solution. The tautomeric forms exhibited a very similar electronic spectra, with bathochromic and hypochromic shifts being observed due to the tautomerization process [L^{2-}(10-O)→L^{2-}(11-O)]. The polarization and specific solute–solvent interaction were observed to be important in the correct description of the electronic transition for the molecules considered in this study.

Acknowledgements

W. B. De Almeida would like to thank the American Chemical Society for a visiting Professor fellowship during his stay at the Quantum Theory Project (QTP) at the University of Florida, and the Sociedade Brasileira de Química for support. W. B. A. also acknowledges the Q.T.P. group for their kind reception. L. R. A. Costa and H. F. Dos Santos thank the Conselho Nacional de Desenvolvimento Científico e Tecnológico (CNPq) for their research grants. This work was supported in part through grants from the office of Naval Research and through NSF Grant CHE 9312651.

References

1 (*a*) A. I. Laskin and J. A. Last, *Antibiot. Chemother.*, 1971, **17**, 1; (*b*) J. J. Stezowski, *J. Am. Chem. Soc.*, 1976, **98**, 6012; (*c*) K. H. Jogun and J. J. Stezowski, *J. Am. Chem. Soc.*, 1976, **98**, 6018; (*d*) H. A. Duarte, MSc Thesis, Depto. de Química, UFMG, 1992.
2 J. M. Siqueria, S. Carvalho, E. B. Paniago, L. Tosi and H. Beraldo, *J. Pharm. Sci.*, 1994, **83**, 291.
3 (*a*) S. V. M. Matos and H. Beraldo, *J. Braz. Chem. Soc.*, 1995, **6**, 405; (*b*) J. M. Siqueira, MSc Thesis, Depto. de Química, UFMG, 1989.
4 G. J. Palenik, M. Mathew and R. Restino, *J. Am. Chem. Soc.*, 1978, **100**, 4458.
5 L. Lambs, B. D.-Le Révérend, H. Kozlowski and G. Berthon, *Inorg. Chem.*, 1988, **27**, 3001.
6 H. F. Dos Santos, W. B. De Almeida and M. C. Zerner, unpublished work.
7 (*a*) J. Ridley and M. C. Zerner, *Theor. Chim. Acta*, 1973, **32**, 111; (*b*) M. C. Zerner, G. H. Loew, R. F. Kirchner and V. T. Mueller-Westerholf, *J. Am. Chem. Soc.*, 1980, **102**, 589; (*c*) J. D. Head and M. C. Zerner, *Chem. Phys. Lett.*, 1986, **131**, 359; (*d*) W. D. Edwalds and M. C. Zerner, *Theor. Chim. Acta*, 1987, **72**, 347.
8 M. M. Karelson and M. C. Zerner, *J. Phys. Chem.*, 1992, **96**, 6949.
9 W. L. Jorgensen, BOSS version 3.5, Biochemical and Organic Simulation System, 1995.
10 (*a*) D. C. Harris and M. D. Bertolucci, *Symmetry and Spectroscopy: An Introduction to Vibrational and Electronic Spectroscopy*, Dover Publication Inc., New York, ch. 5, 1989; (*b*) M. G. Cory, H. Hirose and M. C. Zerner, *Inorg. Chem.*, 1995, **34**, 2969.
11 J. McKelvey, G. Pearl and M. C. Zerner, unpublished work.
12 M. M. Karelson and M. C. Zerner, *J. Am. Chem. Soc.*, 1990, **112**, 9405.

Paper 6/08103G
Received 2*nd December* 1996
Accepted 26*th February* 1997